

# BTeV's Physics Goals and Sensitivities

BTeV Collaboration

May 20, 2004

# Contents

1.1	The CKM Matrix and the CKM Angles . . . . .	1
1.2	Testing for and Defining New Physics . . . . .	2
1.2.1	Generic Tests . . . . .	2
1.2.1.1	A Critical Check Using $\chi$ . . . . .	3
1.2.1.2	Finding Inconsistencies . . . . .	4
1.2.1.3	Generic Tests for New Physics Using Rare Decays . . . . .	4
1.2.2	New Physics Tests in Specific Models . . . . .	5
1.2.2.1	Supersymmetry . . . . .	5
1.2.2.2	Extra Dimensions . . . . .	7
1.2.2.3	SO(10) . . . . .	8
1.2.2.4	Other New Physics Models . . . . .	8
1.2.3	Required Measurements Involving $\beta$ . . . . .	9
1.2.4	Required Measurements Involving $\alpha$ . . . . .	9
1.2.5	Required Measurements Involving $\gamma$ . . . . .	11
1.2.6	Required Measurements Involving $\chi$ . . . . .	12
1.2.7	Conclusions on Importance of $b$ and $c$ Decays . . . . .	13
1.3	BTeV's Physics Reach . . . . .	13
1.3.1	Summary of Flavor Tagging . . . . .	14
1.3.2	Sensitivities to CP Violating Angles . . . . .	14
1.3.3	Sensitivity in Determining $\alpha$ Using $B^0 \rightarrow \rho\pi$ . . . . .	16
1.3.3.1	Event Selection, Event Yields and Backgrounds . . . . .	16
1.3.3.2	Estimation of the Error on $\alpha$ . . . . .	20
1.3.4	Sensitivity to $B_s$ Mixing . . . . .	22
1.3.5	Sensitivities in New Physics Modes . . . . .	22
1.3.5.1	Reach in Rare Decays . . . . .	22
1.3.5.2	Reach in CP Violating Modes . . . . .	24
1.4	Physics Reach of the Stage I Detector and Comparisons with LHCb . . . . .	25
1.4.1	Introduction . . . . .	25

We know that the Standard Model cannot explain the baryon asymmetry of the Universe and problem of extra matter in galaxies, called “Dark Matter.” Therefore, there is New Physics out there that we need to find. There are many other reasons why we believe that the Standard Model is incomplete and there must be physics beyond. One is the plethora of “fundamental parameters,” for example quark masses, mixing angles, etc... The Standard Model cannot explain the smallness of the weak scale compared to the GUT or Planck scales; this is often called “the hierarchy problem.” It is believed that the CKM source of CP violation in the Standard Model is not large enough to explain the baryon asymmetry of the Universe [1]; thus it is very possible that there are large yet unknown CP violation sources that we will discover in  $b$  and/or  $c$  decays. Finally, gravity is not incorporated. John Ellis said “My personal interest in CP violation is driven by the search for physics beyond the Standard Model” [2]. (A more complete description of the basic physics is given in Chapter 1 of our 2002 Proposal Update <http://www-btev.fnal.gov/cgi-bin/public/DocDB/ShowDocument?docid=316> .)

BTeV has many physics goals. The major branches include finding new physics or refining our understanding of new physics found elsewhere, e.g. the LHC, using both CP violating phases and rare  $b$  and  $c$  decays. It is also important to precisely measure Standard Model parameters. Other physics goals include studies of QCD in weak decay processes probed by measuring branching ratios, semileptonic form-factors, polarizations in vector-vector decays and Dalitz plots in three-body decays,  $b$  and  $c$  quark production, structure of  $b$  states including baryon decays and  $B_c$  decays. We fully expect that more than 100 Ph. D. theses will be written on BTeV data.

## 1.1 The CKM Matrix and the CKM Angles

The gauge bosons,  $W^\pm$ ,  $\gamma$  and  $Z^0$  couple to mixtures of the physical  $d$ ,  $s$  and  $b$  states. This mixing is described by the Cabibbo-Kobayashi-Maskawa (CKM) matrix [3]. In the Wolfenstein approximation the matrix is written in order  $\lambda^3$  for the real part and  $\lambda^4$  for the imaginary part as [4]

$$V_{CKM} = \begin{pmatrix} 1 - \lambda^2/2 & \lambda & A\lambda^3(\rho - i\eta)(1 - \lambda^2/2) \\ -\lambda & 1 - \lambda^2/2 - i\eta A^2\lambda^4 & A\lambda^2(1 + i\eta\lambda^2) \\ A\lambda^3(1 - \rho - i\eta) & -A\lambda^2 & 1 \end{pmatrix}. \quad (1.1)$$

The parameters  $\lambda$ ,  $A$ ,  $\rho$  and  $\eta$ , are fundamental constants of nature, just as basic as  $G$ , Newton’s constant, or  $\alpha_{EM}$ . Two are determined from charged-current weak decays. The measured values are  $\lambda = 0.2205 \pm 0.0018$  and  $A = 0.784 \pm 0.043$ . There are constraints on  $\rho$  and  $\eta$  from other measurements. (Usually the matrix is viewed only up to order  $\lambda^3$ . To explain CP violation in the  $K^0$  system the term of order  $\lambda^4$  in  $V_{cs}$  is necessary.)

The unitarity of the CKM matrix allows us to construct six relationships. These may be thought of as triangles in the complex plane shown in Fig. 1.1.

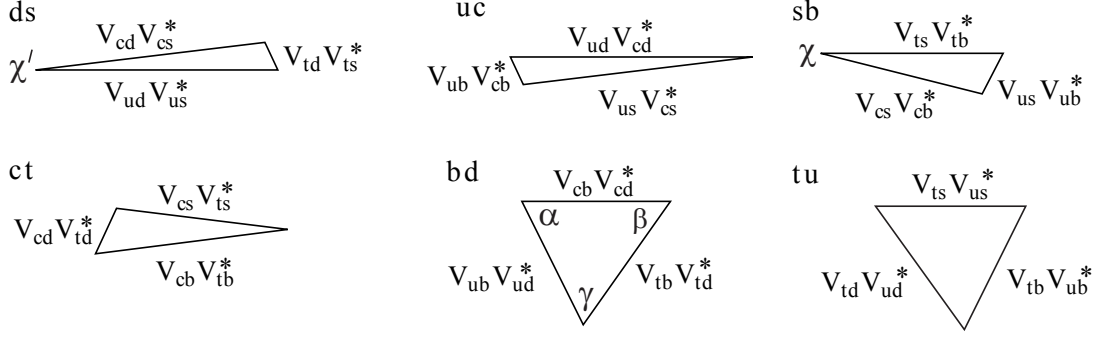


Figure 1.1: The six CKM triangles. The bold labels, e.g. **ds** refer to the rows or columns used in the unitarity relationship. The angles defined in equation (1.2) are also shown.

All six of these triangles can be constructed knowing four and only four independent angles [5][6][7]. These are defined as:

$$\beta = \arg \left( -\frac{V_{tb}V_{td}^*}{V_{cb}V_{cd}^*} \right), \quad \gamma = \arg \left( -\frac{V_{ub}^*V_{ud}}{V_{cb}^*V_{cd}} \right), \quad (1.2)$$

$$\chi = \arg \left( -\frac{V_{cs}^*V_{cb}}{V_{ts}^*V_{tb}} \right), \quad \chi' = \arg \left( -\frac{V_{ud}^*V_{us}}{V_{cd}^*V_{cs}} \right). \quad (1.3)$$

( $\alpha$  can be used instead of  $\gamma$  or  $\beta$ .) Two of the phases  $\beta$  and  $\gamma$  are probably large while  $\chi$  is estimated to be small  $\approx 0.02$ , but measurable, and  $\chi'$  is likely to be much smaller.

The current situation was summarized by Stone [9] (see Fig. 1.2). Here the value  $\sin(2\beta)$  is compared on the  $\rho - \eta$  plane with a fit to measurements of  $|V_{ub}|$  and  $|V_{cb}|$ ,  $\epsilon_K$ , from CP violation in  $K_L$  decay,  $B_d$  mixing and an upper limit on the ratio of  $B_s$  to  $B_d$  mixing. In all measurements but  $\sin(2\beta)$ , the theoretical errors in deriving constraints on  $\rho$  and  $\eta$  from the measurements are dominant.

In performing the fit, the theory parameters are allowed to have equal probability within a restricted but arbitrary range [10]. Therefore, there is a large model dependence for parameter space restricted by measurements of  $(\epsilon_K)$ ,  $|V_{ub}/V_{cb}|$  and  $\Delta m_d$ , with a smaller but significant model dependence for  $\Delta m_s/\Delta m_d$ . The data are surely consistent although the 4-fold ambiguity in  $\beta$ , due to the fact that we measure  $\sin(2\beta)$ , does allow for a rather large surprise.

## 1.2 Testing for and Defining New Physics

### 1.2.1 Generic Tests

We can look for New Physics either in the context of specific models or more generically, for deviations from the Standard Model expectation independent of specific non-standard

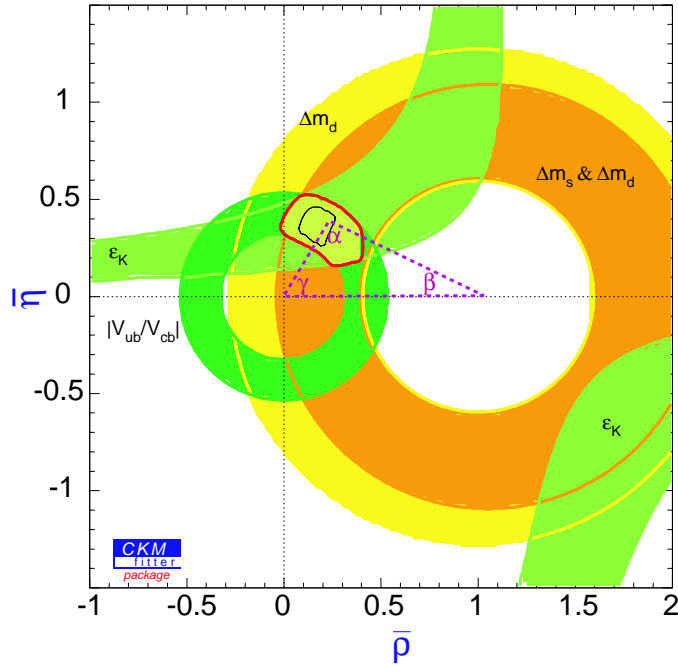


Figure 1.2: Fits in the  $\rho - \eta$  plane using data from CP violation in  $K^0$  decay ( $\epsilon_K$ ),  $|V_{ub}/V_{cb}|$  and the ratio of  $B_s$  mixing ( $\Delta m_s$ ) to  $B_d$  mixing ( $\Delta m_d$ ) compared with the measurement of  $\sin(2\beta)$  from the Babar and Belle collaborations. The angles  $\alpha$ ,  $\gamma$  and one possibility for  $\beta$  are also indicated. ( $\bar{\rho} = \rho(1 - \lambda^2/2)$ , with a similar definition for  $\bar{\eta}$ .) From Stone [9].

models. This can be done for both CP violating decays and rare decays. Let us start with generic tests using CP violation.

### 1.2.1.1 A Critical Check Using $\chi$

It has been pointed out by Silva and Wolfenstein [5] that measuring only angles may not be sufficient to detect new physics. For example, suppose there is new physics that arises in  $B^0 - \bar{B}^0$  mixing. Let us assign a phase  $\theta$  to this new physics. If we then measure CP violation in  $B^0 \rightarrow J/\psi K_s$  and  $B^0 \rightarrow \rho\pi$ , then we actually measure  $2\beta' = 2\beta + \theta$  and  $2\alpha' = 2\alpha - \theta$ . So while there is new physics, we miss it, because  $2\beta' + 2\alpha' = 2\alpha + 2\beta$  and  $\alpha' + \beta' + \gamma = 180^\circ$ .

Measurements of the magnitudes of CKM matrix elements, however, all come with theoretical errors. Some of these are hard to estimate. The best measured magnitude is that of  $\lambda = |V_{us}/V_{ud}| = 0.2205 \pm 0.0018$ . Silva and Wolfenstein [5] [6] show that the Standard Model can be checked in a profound manner by seeing if:

$$\sin \chi = \left| \frac{V_{us}}{V_{ud}} \right|^2 \frac{\sin \beta \sin \gamma}{\sin(\beta + \gamma)} . \quad (1.4)$$

Here the precision of the check will be limited initially by the measurement of  $\sin \chi$ , not of  $\lambda$ .

(BTeV can measure  $\chi$  using the reaction  $B_s \rightarrow J\psi\eta^{(\prime)}$ .) This check can reveal new physics, even if other measurements have not shown any anomalies.

### 1.2.1.2 Finding Inconsistencies

Another interesting way of viewing the physics was given by Peskin [11], and illustrated in Fig. 1.3. Non-Standard Model physics would show up as discrepancies among the values of  $(\rho, \eta)$  derived from independent determinations using CKM magnitudes ( $|V_{ub}/V_{cb}|$  and  $|V_{td}/V_{ts}|$ ), or  $B_d^0$  mixing ( $\beta$  and  $\alpha$ ), or  $B_s$  mixing ( $\chi$  and  $\gamma$ ).

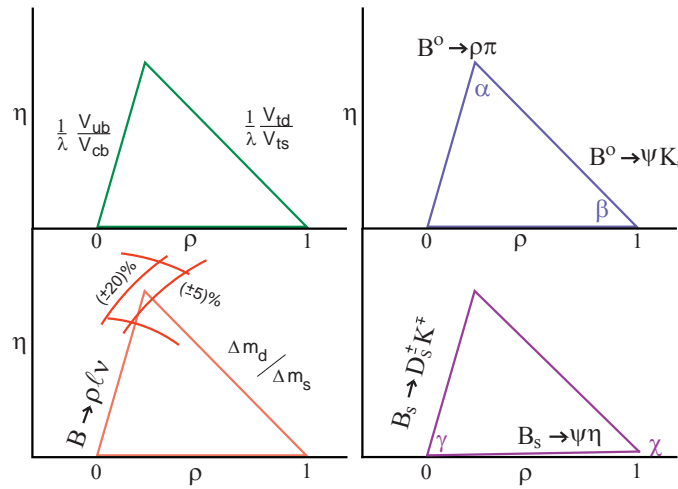


Figure 1.3: One of the CKM triangles showing how it is possible to find the values of  $\eta$  and  $\rho$  using three sets of independent measurements based on CP violating decays going via  $B^0$  mixing (upper right), CP violating decays going via  $B_s$  mixing (lower right), or magnitudes of CKM elements (upper left), with some estimate of the ultimate theoretical errors (lower left). Adopted from Peskin [11].

### 1.2.1.3 Generic Tests for New Physics Using Rare Decays

The basic structure of “Rare  $b$  Decays,” is shown by the loop diagram shown in Fig. 1.4. Here a photon, dilepton pair or gluon can be radiated off any charged particle leg. In the case of the  $\ell^+\ell^-$  pair there can be an intermediate photon or  $Z^0$ . New charged objects can replace quarks and new gauge-like objects can replace the  $W^-$ . Since calculations where the gluon is radiated are more difficult, we will focus mainly on the electromagnetic decays. We consider both inclusive decays such as  $b \rightarrow s\gamma$ ,  $b \rightarrow d\gamma$  and  $b \rightarrow s\ell^+\ell^-$  and their exclusive counterparts,  $B \rightarrow K^*\gamma$ ,  $B \rightarrow \rho\gamma$  and  $B \rightarrow K^*\ell^+\ell^-$ .

Greub, Ioannissian and Wyler [12] write: “.. the decay into  $B \rightarrow K^*\ell^+\ell^-$  yields a wealth of new information on the form of the new interactions since the Dalitz plot is sensitive to subtle interference effects.”

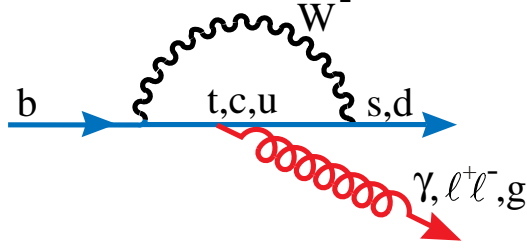


Figure 1.4: Quark level diagram for second order weak processes, often called “penguins” in the literature.

## 1.2.2 New Physics Tests in Specific Models

### 1.2.2.1 Supersymmetry

Supersymmetry is a set of many models. The basic idea is that for every fundamental fermion there is a companion boson and for every boson there is a companion fermion. There are many different implementations of couplings in this framework [13]. In the most general case we pick up 80 new amplitudes and 43 new phases. This is clearly too many to handle so we can try to see things in terms of simpler implementations. In the minimum model (MSSM) we have only two new fundamental phases. One,  $\theta_D$ , would arise in  $B^o$  mixing and the other,  $\theta_A$ , would appear in  $B^o$  decay. A combination would generate CP violation in  $D^o$  mixing, call it  $\phi_{K\pi}$  when the  $D^o \rightarrow K^-\pi^+$  [14]. Table 1.1 shows the CP asymmetry in three different processes in the Standard Model and the MSSM.

Table 1.1: CP Violating Asymmetries in the Standard Model and the MSSM.

Process	Standard Model	New Physics
$B^o \rightarrow J/\psi K_s$	$\sin 2\beta$	$\sin 2(\beta + \theta_D)$
$B^o \rightarrow \phi K_s$	$\sin 2\beta$	$\sin 2(\beta + \theta_D + \theta_A)$
$D^o \rightarrow K^-\pi^+$	0	$\sim \sin \phi_{K\pi}$

Two direct effects of New Physics are clear here. First of all, the difference in CP asymmetries between  $B^o \rightarrow J/\psi K_s$  and  $B^o \rightarrow \phi K_s$  would show the phase  $\phi_A$ . Secondly, there would be finite CP violation in  $D^o \rightarrow K^-\pi^+$  where none is expected in the Standard Model.

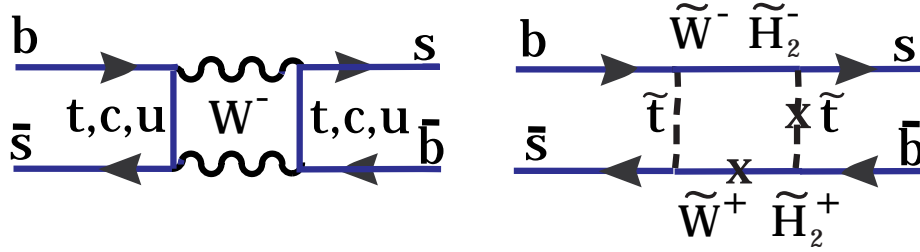
Manifestations of specific SUSY models lead to different patterns. Table 1.2 shows the expectations for some of these models in terms of these variables and the neutron electric dipole moment  $d_N$ ; see [14] for details. Note, that “Approximate CP” has already been ruled out by the measurements of  $\sin 2\beta$ .

Using the MSSM model, Hinchcliff and Kersting predict there will be significant contributions to  $B_s$  mixing, and the CP asymmetry in the charged decay  $B^\mp \rightarrow \phi K^\mp$  [15]. The contribution to  $B_s$  mixing significantly enhances the CP violating asymmetry in modes such

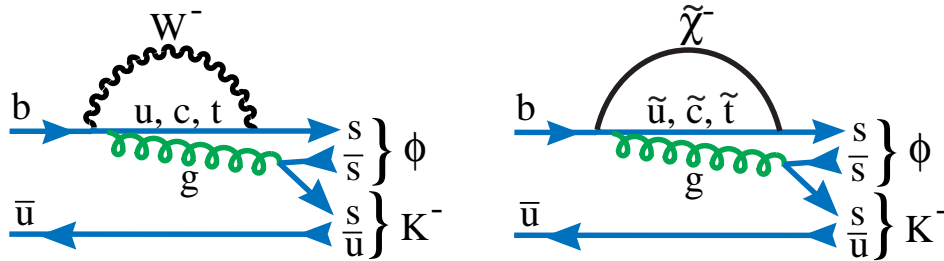
Table 1.2: Some SUSY Predictions.

Model	$d_N \times 10^{-25}$	$\theta_D$	$\theta_A$	$\sin \phi_{K\pi}$
Standard Model	$\leq 10^{-6}$	0	0	0
Approx. Universality	$\geq 10^{-2}$	$\mathcal{O}(0.2)$	$\mathcal{O}(1)$	0
Alignment	$\geq 10^{-3}$	$\mathcal{O}(0.2)$	$\mathcal{O}(1)$	$\mathcal{O}(1)$
Heavy squarks	$\sim 10^{-1}$	$\mathcal{O}(1)$	$\mathcal{O}(1)$	$\mathcal{O}(10^{-2})$
Approx. CP	$\sim 10^{-1}$	$-\beta$	0	$\mathcal{O}(10^{-3})$

as  $B_s \rightarrow J/\psi\eta$ . (Recall the CP asymmetry in this mode is proportional to  $\sin 2\chi$  in the Standard Model.) The Standard Model diagram and MSSM diagrams are shown in Fig. 1.5. The expected CP asymmetry in the MSSM is  $\approx \sin \phi_\mu \cos \phi_A \sin(\Delta m_s t)$ , which is approximately 10 times the expected value in the Standard Model.


 Figure 1.5: The Standard Model (left) and MSSM (right) contributions to  $B_s^0$  mixing.

We observed that a difference between CP asymmetries in  $B^0 \rightarrow J/\psi K_s$  and  $\phi K_s$  arises in the MSSM due to a CP asymmetry in the decay phase. It is possible to observe this directly by looking for a CP asymmetry in  $B^\pm \rightarrow \phi K^\mp$ . The Standard Model and MSSM diagrams are shown in Fig. 1.6. Here the interference of the two diagrams provides the CP asymmetry. The predicted asymmetry is equal to  $(M_W/m_{squark})^2 \sin \phi_\mu$  in the MSSM, where  $m_{squark}$  is the relevant squark mass [15].


 Figure 1.6: The Standard Model (left) and MSSM (right) contributions to  $B^- \rightarrow \phi K^-$ .



The  $\phi K$  and  $\phi K^*$  final states have been observed, first by CLEO [16] and subsequently by BABAR [17]. The average branching ratio is  $\mathcal{B}(B^- \rightarrow \phi K^-) = (6.8 \pm 1.3) \times 10^{-6}$  showing that in principle large samples can be acquired especially at hadronic machines.

The polarization in the rare decay  $B \rightarrow K^* \ell^+ \ell^-$  is also a very effective way of sorting out supersymmetric models. Fig. 1.7 shows the predicted forward-backward polarization as a function of  $s$ , the dilepton invariant mass squared, from Ali *et al.*, [18] for the Standard Model and a collection of supersymmetric models.

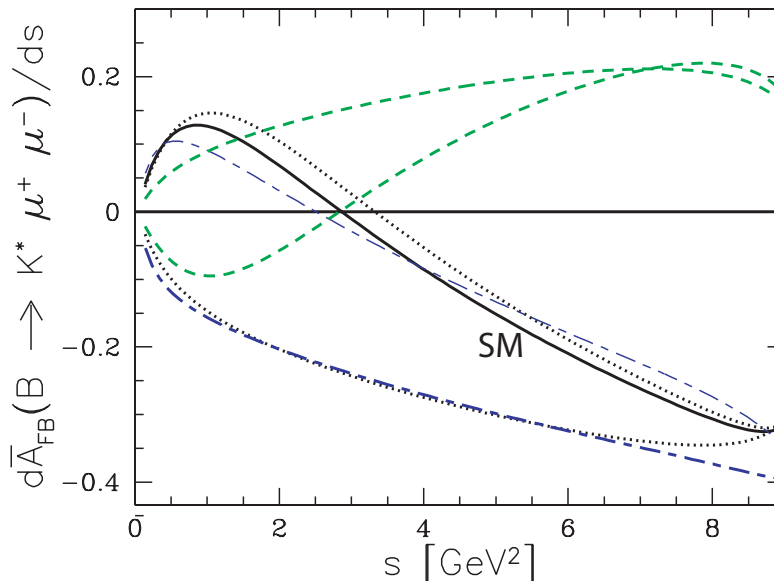


Figure 1.7: The normalized forward-backward asymmetry in  $B \rightarrow K^* \mu^+ \mu^-$  decay as a function of  $s$ , the dilepton invariant mass squared using the form factors from the LCSR approach. The solid line denotes the SM prediction. The dotted (long-short dashed) lines correspond to the SUGRA (the MIA-SUSY) model for different The dashed curves indicating a positive asymmetry for large  $s$  correspond to the MIA-SUSY models for the "best depression scenario." (From ref. [18]).

In a different work, Ali *et al.* tell us: "Precise measurements of the dilepton invariant mass distributions in the decays  $B \rightarrow (s, K^*) \ell^+ \ell^-$  will greatly help in discriminating among the Standard Model and various supersymmetric theories" [19].

### 1.2.2.2 Extra Dimensions

Papers predicting changes in  $B$  decay phenomena when the world has extra physical dimensions are listed in ref. [20]. Another paper by Aranda *et al.* relates quark and neutrino mixing in extra dimensions [21].

Buras *et al.* [22] have considered a model of one universal extra dimension compactified at a scale of  $1/R > 250$  GeV, based on the work of Appelquist, Cheng and Dobrescu (ACD) [23]. The contributions from the Kaluza-Klein modes produce no effect on the major

components now used to determine  $\rho$  and  $\eta$ , namely,  $|V_{ub}/V_{cb}|$ ,  $\Delta m_s/\Delta m_d$  and  $\sin(2\beta)$ . However, there are significant effects on the value of  $V_{td}$ , the size of  $\gamma$  and branching ratio for  $B^0 \rightarrow \mu^+\mu^-$  as shown in Fig. 1.8

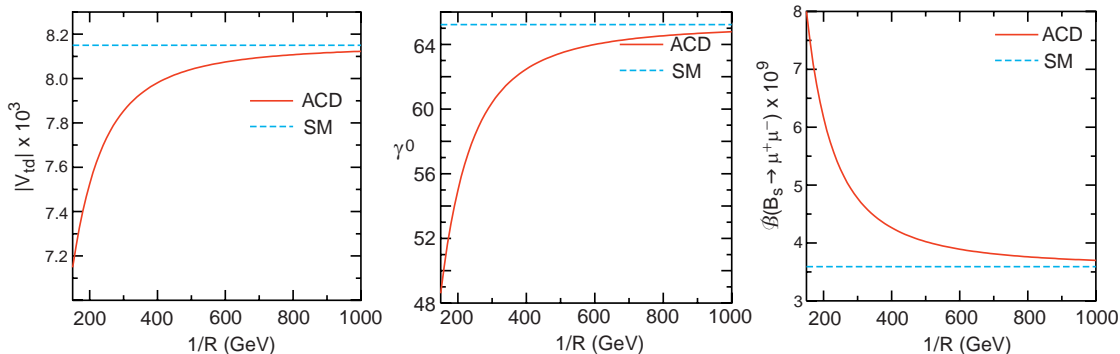


Figure 1.8: The effect on measured quantities of one extra dimension (ACD) compared with the Standard Model (SM) as a function of the compactification scale  $R$ .

More precise measurements are required to differentiate between the Standard Model and this model as  $1/R$  increases.

### 1.2.2.3 SO(10)

A strong connection is made between neutrino mixing and CP violation in the quark sector in a paper by Chang, Masiero and Murayama [24]. In this model the large mixing between  $\nu_\mu$  and  $\nu_\tau$  (from atmospheric neutrino oscillations) can lead to large mixing between  $b_R$  and  $s_R$ . This does not violate any known measurements and leads to large CP violation in  $B_s$  mixing, deviations from  $\sin(2\beta)$  in the reaction  $B^0 \rightarrow \phi K_s$  and changes in the phase  $\gamma$ .

### 1.2.2.4 Other New Physics Models

There are many other specific models that predict New Physics in  $b$  decays. we list here a few of these with a woefully incomplete list of references, to give a flavor of what these models predict.

- *Two Higgs and Multi-Higgs Doublet Models*- They predict large effects in  $\epsilon_K$  and CP violation in  $D^0 \rightarrow K^-\pi^+$  with only a few percent effect in  $B^0$  [14]. Expect to see 1-10% CP violating effects in  $b \rightarrow s\gamma$  [25].
- *Left-Right Symmetric Model*- Contributions compete with or even dominate over Standard Model contributions to  $B_d$  and  $B_s$  mixing. This means that CP asymmetries into CP eigenstates could be substantially different from the Standard Model prediction [14].

- *Extra Down Singlet Quarks*- Dramatic deviations from Standard Model predictions for CP asymmetries in  $b$  decays are not unlikely [14].
- *FCNC Couplings of the  $Z$  boson*- Both the sign and magnitude of the decay leptons in  $B \rightarrow K^* \ell^+ \ell^-$  carry sensitive information on new physics. Potential effects are on the of 10% compared to an entirely negligible Standard Model asymmetry of  $\sim 10^{-3}$  [26].
- *Noncommutative Geometry*- If the geometry of space time is noncommutative, i.e.  $[x_\mu, x_\nu] = i\theta_{\mu\nu}$ , then CP violating effects may be manifest at low energy. For a scale  $< 2$  TeV there are comparable effects to the Standard Model [27].
- *MSSM without new flavor structure*- Can lead to CP violation in  $b \rightarrow s\gamma$  of up to 5% [28]. Ali and London propose [29] that the Standard Model formulas are modified by Supersymmetry as

$$\Delta m_d = \Delta m_d(\text{SM}) \left[ 1 + f \left( m_{\chi_2^\pm}, m_{\tilde{t}_R}, m_{H^\pm}, \tan\beta \right) \right] \quad (1.5)$$

$$\Delta m_s = \Delta m_s(\text{SM}) \left[ 1 + f \left( m_{\chi_2^\pm}, m_{\tilde{t}_R}, m_{H^\pm}, \tan\beta \right) \right] \quad (1.6)$$

$$|\epsilon_K| = \frac{G_F^2 f_K^2 M_K M_W^2}{6\sqrt{2}\pi^2 \Delta M_K} B_K (A^2 \lambda^6 \bar{\eta}) \left[ y_c (\eta_{ct} f_3(y_c, y_t) - \eta_{cc}) + \eta_{tt} y_t f_s(y_t) \left[ 1 + f \left( m_{\chi_2^\pm}, m_{\tilde{t}_R}, m_{H^\pm}, \tan\beta \right) \right] A^2 \lambda^4 (1 - \bar{\rho}) \right] , \quad (1.7)$$

where  $\Delta m(\text{SM})$  refers to the Standard Model formula and the expression for  $|\epsilon_K|$  would be the Standard Model expression if  $f$  were set equal to zero. Ali and London show that it is reasonable to expect that  $0.8 > f > 0.2$ . Since the CP violating angles will not change from the Standard Model, determining the value of  $(\rho, \eta)$  using the magnitudes  $\Delta m_s/\Delta m_d$  and  $|\epsilon_K|$  will show an inconsistency with values obtained using other magnitudes and angles.

### 1.2.3 Required Measurements Involving $\beta$

Besides a more precise measurement of  $\sin 2\beta$  we need to resolve the four ambiguities. There are two suggestions on how this may be accomplished. Kayser [30] shows that time dependent measurements of the final state  $J/\psi K^0$ , where  $K^0 \rightarrow \pi \ell \nu$ , give a direct measurement of  $\cos(2\beta)$  and can also be used for CPT tests. Another suggestion is to use the final state  $J/\psi K^{*0}$ ,  $K^{*0} \rightarrow K_S \pi^0$ , and to compare with  $B_s \rightarrow J/\psi \phi$  to extract the sign of the strong interaction phase shift assuming SU(3) symmetry, and thus determine  $\cos(2\beta)$  [31].

### 1.2.4 Required Measurements Involving $\alpha$

It is well known that  $\sin(2\beta)$  can be measured without problems caused by Penguin processes using the reaction  $B^0 \rightarrow J/\psi K_S$ . The simplest reaction that can be used to measure  $\sin(2\alpha)$

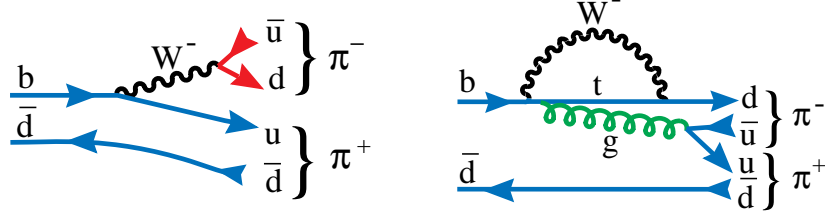


Figure 1.9: Decay diagrams for  $\bar{B}^0 \rightarrow \pi^+\pi^-$ . (left) Via tree level  $V_{ub}$  moderated decay. (right) Via a Penguin process.

is  $B^0 \rightarrow \pi^+\pi^-$ . This reaction can proceed via both the Tree and Penguin diagrams shown in Fig. 1.9.

Current measurements show a large Penguin component. The ratio of Penguin *amplitude* to Tree *amplitude* in the  $\pi^+\pi^-$  channel is about 40% in magnitude. Thus the effect of the Penguin must be determined in order to extract  $\alpha$ . The only model independent way of doing this was suggested by Gronau and London, but requires the measurement of  $B^\mp \rightarrow \pi^\mp \pi^0$  and  $B^0 \rightarrow \pi^0 \pi^0$ , the latter being rather daunting.

There is, however, a theoretically clean method to determine  $\alpha$ . The interference between Tree and Penguin diagrams can be exploited by measuring the time dependent CP violating effects in the decays  $B^0 \rightarrow \rho\pi \rightarrow \pi^+\pi^-\pi^0$  as shown by Snyder and Quinn [32].

The  $\rho\pi$  final state has many advantages. These final states were first seen by CLEO with large rates relative to  $\pi\pi$ . Table 1.3 lists the current measurements.

Table 1.3: Measurements of  $B \rightarrow \rho\pi$  Branching Ratios ( $\times 10^{-6}$ ) or upper limits at 90% confidence level.

Reaction	CLEO [33]	BABAR [34][35]	BELLE [36]	Average
$B^- \rightarrow \rho^0 \pi^-$	$10.4^{+3.3}_{-3.4} \pm 2.1$	$9.5 \pm 1.1 \pm 0.8$	$8.0^{+2.3+0.7}_{-2.0-0.7}$	$9.5 \pm 1.3$
$B^0 \rightarrow \rho^\pm \pi^\mp$	$22.6^{+8.4}_{-7.4} \pm 4.2$	$22.6 \pm 1.8 \pm 2.2$	$29.1^{+5.0}_{-4.9} \pm 4.0$	$23.6 \pm 2.5$
$B^0 \rightarrow \rho^0 \pi^0$	$< 5.5$	$< 2.9$	$6.0^{+2.9}_{-2.3} \pm 1.2$	-

These measurements are consistent with some theoretical expectations [37]. Furthermore, the associated vector-pseudoscalar Penguin decay modes have conquerable or smaller branching ratios. Secondly, since the  $\rho$  is spin-1, the  $\pi$  spin-0 and the initial  $B$  also spinless, the  $\rho$  is fully polarized in the (1,0) configuration, so it decays as  $\cos^2 \theta$ , where  $\theta$  is the angle of one of the  $\rho$  decay products with the other  $\pi$  in the  $\rho$  rest frame. This causes the periphery of the Dalitz plot to be heavily populated, especially the corners. A sample Dalitz plot is shown in Fig. 1.10. This kind of distribution is good for maximizing the interferences, which helps minimize the error. Furthermore, little information is lost by excluding the Dalitz plot interior, a good way to reduce backgrounds.

To estimate the required number of events Snyder and Quinn preformed an idealized analysis that showed that a background-free, flavor-tagged sample of 1000 to 2000 events

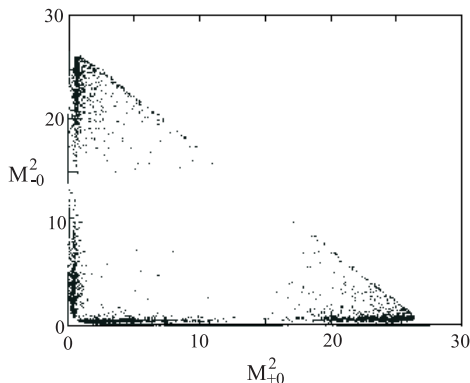


Figure 1.10: The Dalitz plot for  $B^0 \rightarrow \rho\pi \rightarrow \pi^+\pi^-\pi^0$  from Snyder and Quinn.

was sufficient. The 1000 event sample usually yields good results for  $\alpha$ , but sometimes does not resolve the ambiguity. With the 2000 event sample, however, they always succeeded.

This technique not only finds  $\sin(2\alpha)$ , it also determines  $\cos(2\alpha)$ , thereby removing two of the remaining ambiguities. The final ambiguity can be removed using the CP asymmetry in  $B^0 \rightarrow \pi^+\pi^-$  and a theoretical assumption [38].

### 1.2.5 Required Measurements Involving $\gamma$

It may be easier to measure  $\gamma$  than  $\alpha$  in a model independent manner. There have been two methods suggested.

(1) Time dependent flavor tagged analysis of  $B_s \rightarrow D_s^\pm K^\mp$ . This is a direct model independent measurement [39]. Here the Cabibbo suppressed  $V_{ub}$  decay interferes with a somewhat less suppressed  $V_{cb}$  decay via  $B_s$  mixing as illustrated in Fig. 1.11 (left). Even though we are not dealing with CP eigenstates here there are no hadronic uncertainties, though there are ambiguities. Since this proceeds via  $B_s$  mixing the exact CP violating angle measured is  $\gamma - 2\chi$ .

(2) Measure the rate differences between  $B^- \rightarrow \overline{D}^0 K^-$  and  $B^+ \rightarrow D^0 K^+$  in two different  $D^0$  decay modes such as  $K^-\pi^+$  and  $K^+K^-$ . This method makes use of the interference between the tree and doubly-Cabibbo suppressed decays of the  $D^0$ , and does not depend on any theoretical modeling [40][41]. See Fig. 1.11 (right).

Several model dependent methods using the light two-body pseudoscalar decay rates have been suggested for measuring  $\gamma$ . The basic idea in all these methods can be summarized as follows:  $B^0 \rightarrow \pi^+\pi^-$  has the weak decay phase  $\gamma$ . In order to reproduce the observed suppression of the decay rate for  $\pi^+\pi^-$  relative to  $K^\pm\pi^\mp$  we require a large negative interference between the Tree and Penguin amplitudes. This puts  $\gamma$  in the range of  $90^\circ$ . There is a great deal of theoretical work required to understand rescattering, form-factors etc... We are left with several ways of obtaining model dependent limits, due to Fleischer and Mannel [42], Neubert and Rosner [43], Fleischer and Buras [44], and Beneke *et al.* [45]. The latter make a sophisticated model of QCD factorization and apply corrections. These ideas may

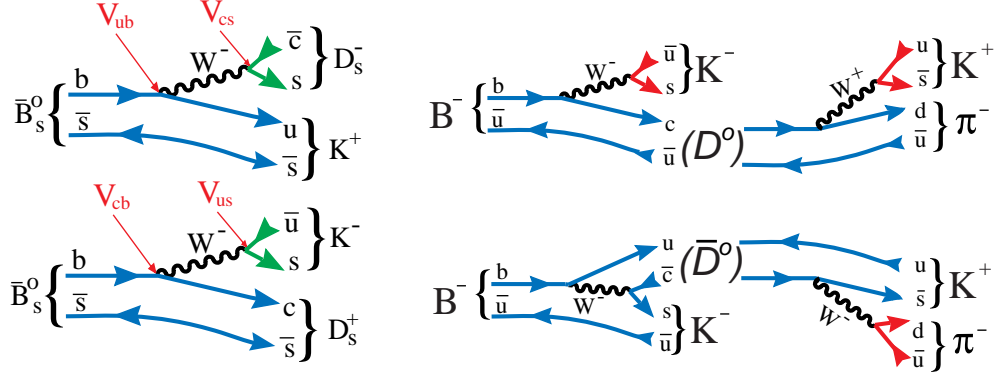


Figure 1.11: (left) The two diagram diagrams for  $B_s \rightarrow D_s^\pm K^\mp$  that interfere via  $B_s$  mixing. (right) The two interfering decay diagrams for  $B^- \rightarrow \bar{D}^0 K^-$  where one is a  $b \rightarrow u$  transition and the other a doubly-Cabibbo suppressed decay.

be very useful for resolving ambiguities, but the amount of model dependence will remain a concern.

Another method for determining  $\gamma$  proposed by Fleischer [46] uses the assumption of U-spin symmetry ( $d \longleftrightarrow s$ ) and requires the measurement of both  $B^0 \rightarrow \pi^+ \pi^-$  and  $B_s \rightarrow K^+ K^-$  CP asymmetries. Again the model dependence here is a concern, but it may be quite useful for ambiguity resolution.

### 1.2.6 Required Measurements Involving $\chi$

The angle  $\chi$ , defined in equation 1.2, can be extracted by measuring the time dependent CP violating asymmetry in the reaction  $B_s \rightarrow J/\psi \eta^{(\prime)}$ , or if one's detector is incapable of quality photon detection, the  $J/\psi \phi$  final state can be used. However, in this case there are two vector particles in the final state, making this a state of mixed CP, requiring a time-dependent angular analysis to extract  $\chi$ , that requires large statistics. Fig. 1.12 shows the decay diagram.

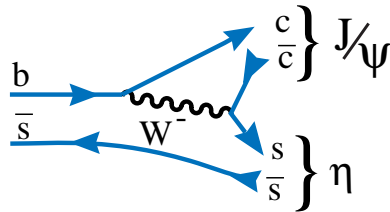


Figure 1.12: The decay diagram for  $B_s \rightarrow J/\psi \eta$ . The final state is a CP eigenstate.

Once  $\chi$ ,  $\beta$  and  $\alpha$  or  $\gamma$  are precisely measured, then all the magnitudes of the CKM elements can be determined. The only model dependent theoretical error arises from the determination of  $\lambda$ , of the order of 1% [6].

### 1.2.7 Conclusions on Importance of $b$ and $c$ Decays

It is clear that precision studies of CP violating  $B_s$ ,  $B^0$  and  $D^0$  decays, and rare decays, can bring a wealth of information to bear on new physics, that probably will be crucial in sorting out anything seen at the LHC. A picture of the effects on  $b$  physics by Hiller is illustrative and shown in Fig. 1.13 [47].

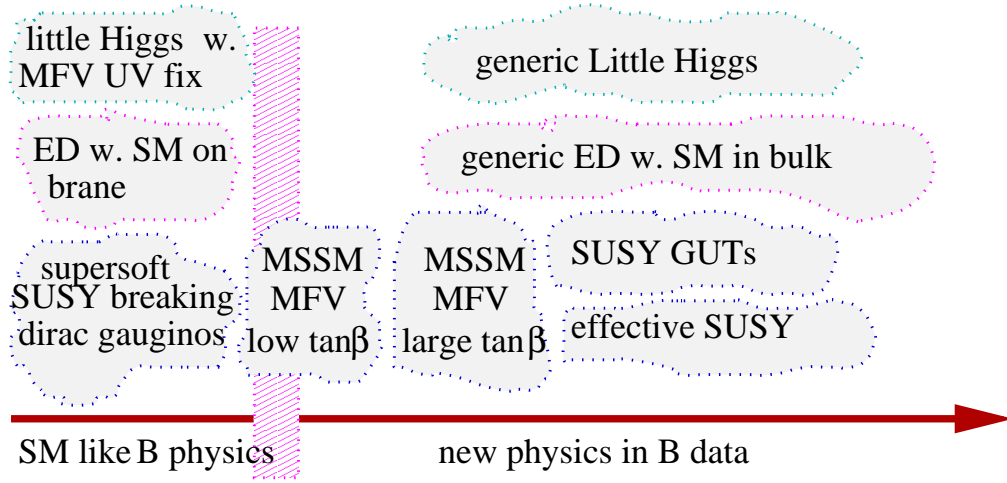


Figure 1.13: Effects on rare or CP violating  $B$  decays from different models of Electroweak symmetry breaking. (From Hiller [47].)

The connections of our physics studies with other experiments in the LHC era sketched in Fig. 1.14. Our studies of CP violation and rare decays will play a central role in sorting out new physics and providing clues to the flavor puzzle along with neutrino physics.

We close this section with a quote from Masiero and Vives [48]: “The relevance of SUSY searches in rare processes is not confined to the usually quoted possibility that indirect searches can arrive ‘first’ in signaling the presence of SUSY. Even after the possible direct observation of SUSY particles, the importance of FCNC and CP violation in testing SUSY remains of utmost relevance. They are and will be complementary to the Tevatron and LHC establishing low energy supersymmetry as the response to the electroweak breaking puzzle.”

We agree, except that we would replace “SUSY” with “New Physics.”

## 1.3 BTeV’s Physics Reach

We will now show that BTeV is well equipped to address all of the issues discussed above. BTeV can also investigate many other physics topics that we have not mentioned that may turn out to be of great import in the future, for example CPT violation [49].

The results quoted here are based on the tools described and studies reported in Part III, “Physics Simulations” of the May, 2000 BTeV proposal [50]. These studies were rigorous and extensive. In most case GEANT3 was used, where both signal events and background

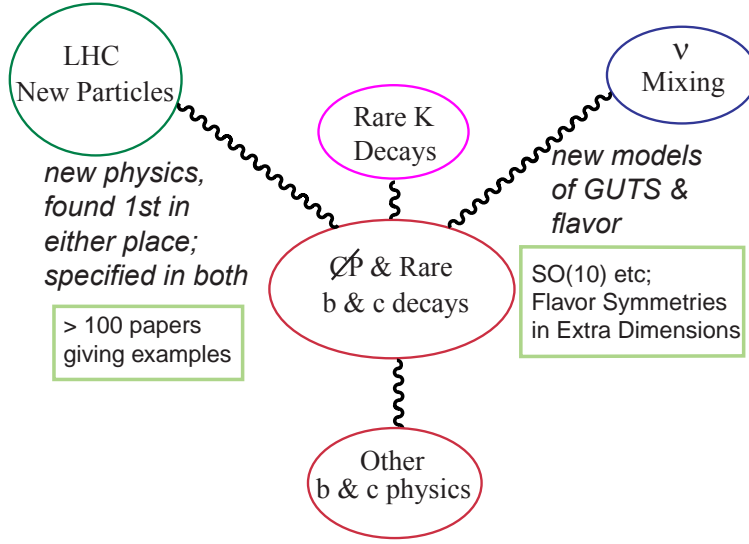


Figure 1.14: Links between studies of CP violation in  $b$  and  $c$  decays with searches for new phenomena at the LHC and experiments in the neutrino sector.)

samples  $\sim 10^7$  events were generated and reconstructed. These simulation results reflect those presented in our 2002 Proposal Update, for the most part, although there have been some additions and corrections due to further analysis.

### 1.3.1 Summary of Flavor Tagging

A detailed study of flavor tagging is given in the 2002 Proposal Update in section 2.10 (page 20 of Chapter 2). There we showed that we can achieve an effective flavor tagging efficiency, characterized as the product of the efficiency  $\epsilon$  and the dilution  $D$  as  $\epsilon D^2$  of 10% for  $B^0$  decays. This study also shows that, as expected,  $B_s$  decays have higher tagging efficiency because of the charged kaon produced to conserve flavor in the  $b$  quark fragmentation to a  $B_s$ . This “same side” tagging is quite favorable and, as a result, we achieve 13% for  $\epsilon D^2$  in  $B_s$  decays.

### 1.3.2 Sensitivities to CP Violating Angles

BTeV will have outstanding performance in determining CP violating asymmetries. The results of our simulations are summarized in Table 1.4 for a luminosity of  $2 \times 10^{32} \text{ cm}^{-2}\text{s}^{-1}$  and  $10^7$  seconds of running time. Descriptions of the analysis techniques used to obtain the signal and background yields are given in the BTeV Proposal.

All of the measurements listed here to determine  $\chi$ ,  $\alpha$ ,  $\beta$ ,  $\gamma$  and  $x_s$ , except for the determination of  $\gamma$  using the  $B \rightarrow K\pi$  modes, are completely free of hadronic uncertainties or errors due to theoretical models. Ultimately, at the level of errors below  $1^\circ$  for  $\alpha$ ,  $\beta$  and  $\gamma$  (and a much lower number for  $\chi$ ), the effects of other diagrams or higher order terms in the



Table 1.4: Yearly sensitivities to CP violating angles and related quantities. (Reactions between lines are used together.)

Reaction	$\mathcal{B} \times 10^{-6}$	# of Events	S/B	Parameter	Error (Value)
$B_s \rightarrow D_s^+ K^-$	300	7,500	7	$\gamma - 2\chi$	$8^\circ$
$B_s \rightarrow D_s^+ \pi^-$	3000	59,000	3	$x_s$	(75)
$B^0 \rightarrow J/\psi K_s$	445	168,000	10	$\sin(2\beta)$	0.017
$B^0 \rightarrow J/\psi K^0$					
$K^0 \rightarrow \pi^\pm \ell^\mp \nu$	7	250	2.3	$\cos(2\beta)$	$\sim 0.5$
$B^0 \rightarrow \pi^+ \pi^-$	4.5	14,600	3	Asymmetry	0.030
$B_s \rightarrow K^+ K^-$	17	18,900	6.6	Asymmetry <sup>†</sup>	0.020
$B^- \rightarrow \bar{D}^0 (K^+ \pi^-) K^-$	0.17	170	1		
$B^- \rightarrow \bar{D}^0 (K^+ K^-) K^-$	1.1	1000	$>10$	$\gamma$	$13^\circ$
$B^- \rightarrow K_s \pi^-$	12.1	4,600	1		$< 4^\circ +$
$B^0 \rightarrow K^+ \pi^-$	18.8	62,100	20	$\gamma$	theory errors
$B^0 \rightarrow \rho^+ \pi^-$	28	5,400	4.1		
$B^0 \rightarrow \rho^0 \pi^0$	5	780	0.3	$\alpha$	$\sim 4^\circ$
$B_s \rightarrow J/\psi \eta$	330	2,800	15		
$B_s \rightarrow J/\psi \eta'$	670	9,800	30	$\sin(2\chi)$	0.024

<sup>†</sup> Can be used for a model dependent estimate of  $\gamma$ , see ref. [46].

Wolfenstein approximation need to be considered. We are now far from this level of concern.

There are other ways to determine some of these angles that we have not discussed. Omission from this table, does not necessarily imply that we cannot use a particular technique, but merely that we have not yet simulated or completely considered the implications of that method. For example, measuring the CP asymmetry in the decay  $B^0 \rightarrow D^{*+} \pi^-$  has been shown to be a model independent way of measuring  $(-2\beta - \gamma)$  [51]. On the other hand, the physical asymmetry is expected to be below 1%, making systematic errors in the efficiencies of detecting positive versus negative tracks, particularly the pion from the  $D^{*+}$  decay, a key issue. We simply have not yet evaluated this tantalizing approach.

We briefly discuss some of these measurements:

- We use the method proposed by Snyder and Quinn to determine  $\alpha$  using  $B^0 \rightarrow \rho \pi \rightarrow \pi^+ \pi^- \pi^0$  [52]. Both the signal efficiencies and the background levels were determined by a full GEANT simulation. We give details on our study that estimated the error in  $\alpha$  below. Quinn and Silva have proposed using non-flavor-tagged rates as input to improve the accuracy of the  $\alpha$  determination [53]. We have not yet incorporated this idea.
- Although the  $B \rightarrow K \pi$  modes provide the smallest experimental error in determining  $\gamma$ , there are model dependent errors associated with this method. On the other hand, two

other methods, which use  $B_s \rightarrow D_s^\pm K^\mp$  and  $B^- \rightarrow \bar{D}^0 K^-$ , provide model independent results and can be averaged. The interplay of the three methods can be used to resolve ambiguities.

- The error in  $\sin(2\chi)$  averaged over both  $J/\psi\eta$  and  $J/\psi\eta'$  decay modes of the  $B_s$  is  $\pm 0.024$ . This translates to an error in the angle  $\chi$  of  $0.7^\circ$ . Since  $\chi$  is expected to be  $\sim 2^\circ$ , a precision measurement will take a few years if it is in the Standard Model range. Including  $B_s \rightarrow J/\psi\phi$  can help reduce the time.
- The asymmetry in  $B^0 \rightarrow \pi^+\pi^-$  may be useful to gain insight into the value of  $\alpha$  with theoretical input or combined with  $B_s \rightarrow K^+K^-$  and theory to obtain  $\gamma$ . This study was done both with MCFast and GEANT. The signal efficiency is 10% higher in MCFast and the background levels the same in both, within statistics.
- The sign of  $\cos(2\beta)$  can be determined in a few years without any theoretical assumptions using  $B^0 \rightarrow J/\psi K^0$ , with  $K^0 \rightarrow \pi^\pm \ell^\mp \nu$ , allowing the removal of two of the ambiguities in  $\beta$ . This reaction can also be used for CPT tests.

### 1.3.3 Sensitivity in Determining $\alpha$ Using $B^0 \rightarrow \rho\pi$

#### 1.3.3.1 Event Selection, Event Yields and Backgrounds

Here we give a detailed explanation of how the error in  $\alpha$  was evaluated as an example of our analysis procedures as documented in the BTeV Proposal and the Proposal Update [55]. To measure  $\alpha$  using  $B^0 \rightarrow \rho\pi$  requires the measurement of the tagged, time-dependent CP asymmetry in a particular combination of amplitudes obtained from a Dalitz plot analysis of the decay. The combination of amplitudes causes the Penguin terms to cancel and isolates the tree contribution to the decay, which provides the value of  $\alpha$ . We have performed a Dalitz plot analysis that includes detector resolution and background along with the expected levels of detected signal events.

The reconstruction efficiencies for  $B \rightarrow \rho\pi$  and backgrounds were studied using a full GEANT simulation, for  $\rho^\pm\pi^\mp$  and  $\rho^0\pi^0$ , separately. All signal and background samples were generated with a mean of two interactions per crossing. relatively easy to generate, it is difficult to generate adequate samples of background events. For channels with branching ratio's of the order of  $10^{-5}$ , it is necessary to generate  $\sim 10^7$  events.

We look for events containing a secondary vertex formed by two oppositely charged tracks. One of the most important selection requirements for discriminating the signal from the background is that the events have well measured primary and secondary vertices. We demand that both the primary and the secondary have vertex fits with  $\chi^2/dof < 2$ . We also make a cut on the the distance between the primary and the secondary vertices, divided by the error,  $L/\sigma_L > 4$ . The two vertices must also be separated from each other in the plane transverse to the beam. We define  $r_{transverse}$  in terms of the primary interaction vertex position  $(x_P, y_P, z_P)$  and the secondary decay vertex position  $(x_S, y_S, z_S)$  as  $r_{transverse} = \sqrt{(x_P - x_S)^2 + (y_P - y_S)^2}$  and cut out events where the secondary vertex is close to the

reconstructed primary. Furthermore, to insure that the charged tracks do not originate from the primary, we require that both the  $\pi^+$  and the  $\pi^-$  candidate have an impact parameter with respect to the primary vertex (DCA)  $> 100 \mu\text{m}$ .

Events passing these selection criteria are searched for good  $\pi^0$  candidates. We select “bumps” in the calorimeter using cluster finder code that does the full pattern recognition. Photon candidates are required to have a minimum bump energy of 1 GeV and pass the shower “shape” cut which requires  $E9/E25 > 0.85$ , this selection is almost fully efficient on real electromagnetic showers and rejects backgrounds from hadronic interactions. We further reduce the background by ensuring that the photon candidates are not too close to the projection of any charged tracks on the calorimeter. For  $\rho^\pm\pi^\mp$ , the minimum distance requirement is  $> 2 \text{ cm}$ , while for  $\rho^0\pi^0$ , we require the minimum distance  $> 5.4 \text{ cm}$ . Candidate  $\pi^0$ 's are two-photon combinations with invariant mass between 125 and 145  $\text{MeV}/c^2$ . More details of  $\pi^0$  selection are given in the description of the analysis of the channel  $B^0 \rightarrow D^{*-}\rho^+$  in Section 16.3 of the 2002 Proposal.

Kinematic cuts greatly reduce the background to  $B \rightarrow \rho\pi$  while maintaining the signal efficiency. Minimum energy and transverse momentum ( $p_t$ ) requirements are placed on each of the three pions. Here  $p_t$  is defined with respect to the  $B$  direction which is defined by the position of the primary and secondary vertices. We demand that the momentum vector of the reconstructed  $B$  candidate point back to the primary vertex. The cut is implemented by requiring  $p_t$  balance among the  $\pi^+$  plus  $\pi^-$ , and  $\pi^0$  candidates relative to the  $B$ -direction and then divided by the sum of the  $p_t$  values for all three particles ( $\Delta p_t/\Sigma p_t$ ). We also make a cut on the  $B$  decay time requiring that the  $B$  candidate live no more than 5.5 proper lifetimes ( $t_{\text{proper}}/t_0 < 5.5$ ). The selection criteria for the two modes are summarized in Table 1.5.

For this study, we generated and analyzed three large samples of events using BTeVGeant: 250,000  $B \rightarrow \rho^0\pi^0$  events, 250,000  $B \rightarrow \rho^+\pi^-$  events, and 9,900,000 generic  $b\bar{b}$  background events. Background from minimum bias events has been shown to be negligible. The results of the analysis after applying the cuts in Table 1.5 are presented in Fig. 1.15 (for  $\rho^0\pi^0$ ) and Fig 1.16 (for  $\rho^+\pi^-$ ). The background mass spectra are on the left side of the figures, and the signal events are on the right side.

The mass resolution for the  $B$  is  $\approx 28 \text{ MeV}/c^2$ . The mean  $\pi^0$  mass value in the  $B \rightarrow \rho\pi$  events is  $135 \text{ MeV}/c^2$  with a resolution of about  $3 \text{ MeV}/c^2$ . The relevant yields for  $\rho\pi$  are shown in Table 1.6. The reconstruction efficiency is  $(0.18 \pm 0.01)\%$  for  $\rho^0\pi^0$  and  $(0.22 \pm 0.01)\%$  for  $\rho^+\pi^-$ . The background was obtained by considering the mass interval between 5 and 7  $\text{GeV}/c^2$ . The signal interval is taken as  $\pm 2\sigma$  around the  $B$  mass or  $112 \text{ MeV}/c^2$ .

The final numbers of both signal and background events are reduced by including the Level 1 and Level 2 trigger efficiency, but the S/B ratio is not significantly changed. From this study we find that we can expect to reconstruct 5,400  $\rho^\pm\pi^\mp$  events and 776  $\rho^0\pi^0$  events per year.

We can, therefore, expect to collect a sample of 540 flavor tagged  $\rho^\pm\pi^\mp$  events and  $\sim 78$   $\rho^0\pi^0$  per year with signal-to-background levels of approximately 4:1 and 1:3, respectively.

Table 1.5: Selection Criteria

Criteria	$\rho^{\pm}\pi^{\mp}$	$\rho^0\pi^0$
Primary vertex criteria	$\chi^2 < 2$	$\chi^2 < 2$
Secondary vertex criteria	$\chi^2 < 2$	$\chi^2 < 2$
$r_{transverse}$ (cm)	0.0146	0.0132
Normalized distance $L/\sigma$	$> 4$	$> 4$
Distance $L$ , cm	$< 5$	$< 5$
DCA of track, $\mu\text{m}$	$> 100$	$> 100$
$t_{proper}/t_0$	$< 5.5$	$< 5.5$
$E_{\pi^+}$ , GeV	$> 4$	$> 4$
$E_{\pi^-}$ , GeV	$> 4$	$> 4$
$p_t(\pi^+)$ , GeV/ $c$	$> 0.4$	$> 0.4$
$p_t(\pi^-)$ , GeV/ $c$	$> 0.4$	$> 0.4$
Isolation for $\gamma$ , cm	$> 2.0$	$> 5.4$
$E_{\pi^0}$ , GeV	$> 5$	$> 9$
$p_t(\pi^0)$ , GeV/ $c$	$> 0.75$	$> 0.9$
$\Delta p_t/\Sigma p_t$	$< 0.06$	$< 0.066$
$m_{\pi^0}$ , MeV/ $c^2$	125 – 145	125 – 145
$m_{\rho}$ , GeV/ $c^2$	0.55 – 1.1	0.55 – 1.1

Table 1.6:  $B \rightarrow \rho\pi$  Yields

Quantity	$\rho^{\pm}\pi^{\mp}$	$\rho^0\pi^0$
Branching ratio	$2.8 \times 10^{-5}$	$0.5 \times 10^{-5}$
Efficiency	0.0022	0.0018
Trigger efficiency (Level 1)	0.7	0.7
Trigger efficiency (Level 2)	0.9	0.9
S/B	4.1	0.3
Signal/ $10^7$ s	5,400	776
$\epsilon D^2$	0.10	0.10
Flavor tagged yield	540	78

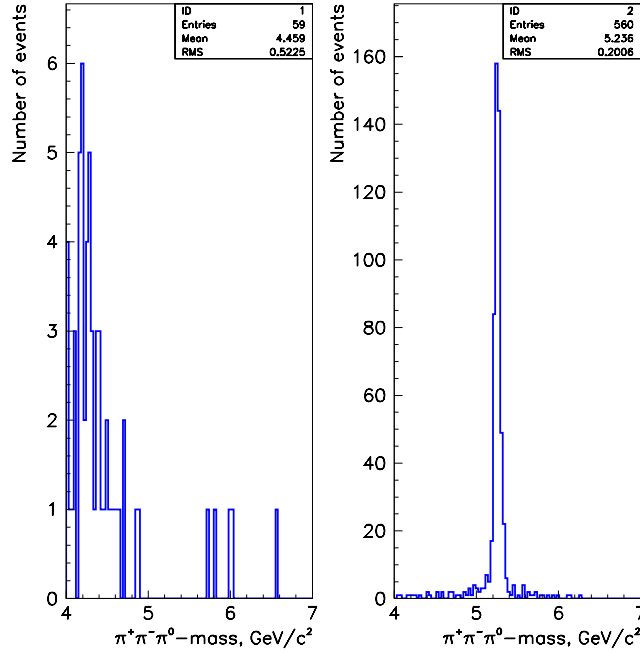


Figure 1.15: Invariant  $\pi^+\pi^-\pi^0$  mass distributions for background (left) and signal (right) events for  $B \rightarrow \rho^0\pi^0$ .

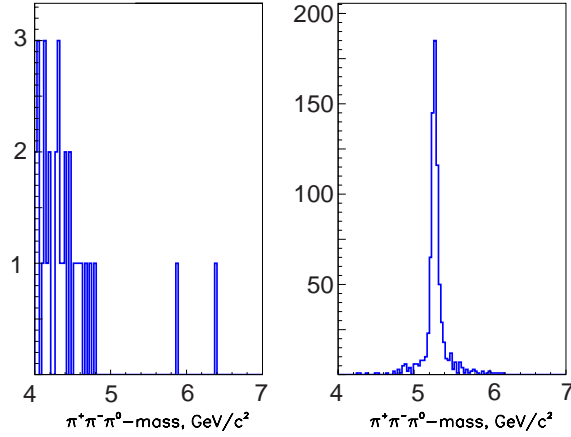


Figure 1.16: Invariant  $\pi^+\pi^-\pi^0$  mass distributions for background (left) and signal (right) events for  $B \rightarrow \rho^+\pi^-$ .

### 1.3.3.2 Estimation of the Error on $\alpha$

The decay amplitude may be written as

$$|B^0\rangle = f_+ a_{+-} + f_- a_{-+} + f_0 a_{00},$$

where  $a_{i,j}$  refers to the three distinct final states as

$$a_{i,j} = a(B^0 \rightarrow \rho^i \pi^j), \quad (i,j) = (+,-), (-,+), (0,0),$$

and  $f_k$  parameterizes the  $\rho$  decay amplitude. We use

$$f_k(s) = \frac{\cos \theta_k}{s - m_\rho^2 + i \prod(s)},$$

where  $\theta_k$  is the angle between the direction of the  $B$  and the direction of a daughter pion, both viewed in the  $\rho$  rest frame, and  $s$  is the square of the dipion invariant mass  $s = (E_{\pi_1} + E_{\pi_2})^2 - (\vec{p}_{\pi_1} + \vec{p}_{\pi_2})^2$ ;  $s$  can be in one of three charge states,  $s^+$ ,  $s^-$  or  $s^0$ . In each case

$$\prod(s) = \frac{m_\rho^2}{\sqrt{s}} \left( \frac{p(s)}{p(m_\rho^2)} \right)^3 \Gamma_\rho(m_\rho^2),$$

$p$  being the momentum in the  $\rho$  rest frame.

The amplitudes  $a_{i,j}$  for  $B^0$  and  $\bar{B}^0$  decay are written as a sum of Tree ( $T$ ) and Penguin ( $P$ ) parts as

$$\begin{aligned} a_{+-} &= -e^{i\gamma} T^{+-} + e^{-i\beta} P^{+-} \\ a_{-+} &= -e^{i\gamma} T^{-+} + e^{-i\beta} P^{-+} \\ a_{00} &= -e^{i\gamma} T^{00} + e^{-i\beta} P^{00} \\ \bar{a}_{+-} &= -e^{-i\gamma} T^{-+} + e^{i\beta} P^{-+} \\ \bar{a}_{-+} &= -e^{-i\gamma} T^{+-} + e^{i\beta} P^{+-} \\ \bar{a}_{00} &= -e^{-i\gamma} T^{00} + e^{i\beta} P^{00}, \end{aligned}$$

where  $\gamma$  and  $\beta$  are the usual CKM angles and  $\alpha + \beta + \gamma = \pi$ . Using both isospin symmetry and the fact that the Penguin amplitude is a pure  $\Delta I = 1/2$  transition leads to the replacement

$$P^{00} = -\frac{1}{2}(P^{+-} + P^{-+}).$$

This leaves us with 9 parameters to be fit to the data including  $\alpha$ , 3 complex Tree and 2 Penguin amplitudes, where one is defined as purely real and the total rate is used as an independent input. We can also allow the resonant and non-resonant background fractions to be determined by the fit, which adds two additional parameters.

For this study we used a data sample corresponding to 1.4 years of running ( $1.4 \times 10^7$ s) with the one-arm version of BTeV. The background level is determined by a full

GEANT simulation of 9,900,000 generic  $b\bar{b}$  events; it is assumed that this background has an exponential time dependence given by the average lifetime of  $b$ -flavored hadrons. The background is parameterized with both resonant and non-resonant components. The non-resonant background is distributed uniformly over the Dalitz plot. The resonant background allows for two of the pions to have a Breit-Wigner shaped low mass enhancement. All charged tracks and photons in both signal and background events are smeared by the detector resolution before further analysis. Signal events are generated with an exponential time distribution modified by  $B^o$  mixing. The simulation is repeated for different assumptions about the relative size of Penguin and Tree amplitudes and the fraction of resonant and non-resonant background. For each set of data a maximum likelihood fit is performed where the likelihood is given by

$$\begin{aligned}
-2 \ln \mathcal{L} = & -2 \sum_{i=1}^{N_{B^o}} \ln \left[ \left( \frac{|\mathcal{A}(s_i^+, s_i^-, t_i; \alpha, ..)|^2}{\mathcal{N}(\alpha, ..)} \times \varepsilon(s_i^+, s_i^-) + \right. \right. \\
& R_{non} \times \frac{1}{\mathcal{N}_t} + R_{res} \times \frac{|\mathcal{BW}(s_i^+, s_i^-)|^2}{\mathcal{N}_{BW}} \times \varepsilon(s_i^+, s_i^-) \Big) / (1 + R_{non} + R_{res}) \Big] \\
& -2 \sum_{j=1}^{N_{\bar{B}^o}} \ln \left[ \left( \frac{|\bar{\mathcal{A}}(s_j^+, s_j^-, t_j; \alpha, ..)|^2}{\mathcal{N}(\alpha, ..)} \times \varepsilon(s_j^+, s_j^-) + \right. \right. \\
& R_{non} \times \frac{1}{\mathcal{N}_t} + R_{res} \times \frac{|\mathcal{BW}(s_j^+, s_j^-)|^2}{\mathcal{N}_{BW}} \times \varepsilon(s_j^+, s_j^-) \Big) / (1 + R_{non} + R_{res}) \Big],
\end{aligned}$$

where  $N_{B^o}$  and  $N_{\bar{B}^o}$  are the total number of  $B^o$  and  $\bar{B}^o$  events, respectively, and  $\mathcal{N}$  is the normalization. It is given by  $(|\mathcal{A}|^2 + |\bar{\mathcal{A}}|^2) \times \varepsilon$ , integrated over the Dalitz plot acceptance, where  $\varepsilon$  is the detector efficiency.  $R_{non}$  and  $R_{res}$  are the ratios of non-resonant and resonant background to signal. For one case we show in Fig. 1.17 the  $\chi^2$  contours for  $\alpha$  and correlations with the fractions of resonant and non-resonant backgrounds. The input value for  $\alpha$  in this case was  $77.3^\circ$ . The fit has no trouble picking out the correct solution.

Table 1.7 shows the results of an ensemble of fits with different assumptions on the fractions of resonant and non-resonant background, and different values of  $\alpha$ . The one parameter fit assumes that the non-resonant and resonant background levels are determined from non-flavor tagged data, while in the three parameter fit, these are determined along with  $\alpha$ .

These studies show that over a broad range of background models,  $\alpha$  is determined with a sensitivity between  $1.4^\circ$ - $4.3^\circ$  in  $1.4 \times 10^7$ s of running time. The sensitivity will also depend on several unknown quantities including the branching ratio for  $\rho^o \pi^o$ , and the ratio of Tree to Penguin amplitudes, though this ratio has been inferred from the branching rates measured for two-body vector-pseudoscalar final states, and reasonable variations have already been included in these sensitivity estimates.

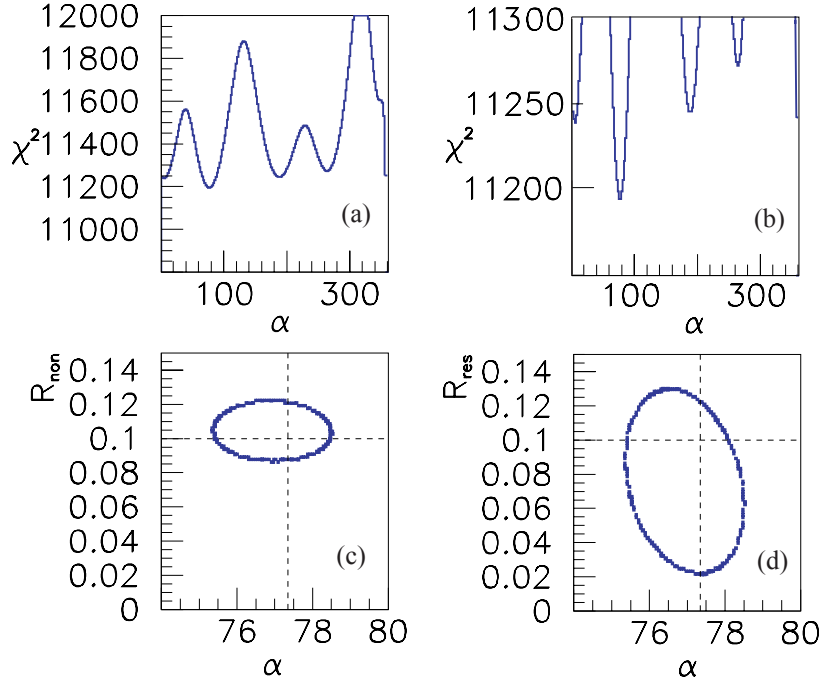


Figure 1.17: Results of a simulation using 1000  $B^0 \rightarrow \rho\pi$  detected signal events with an input value of  $\alpha = 77.3^\circ$ . (a) The  $\chi^2$  contours as a function of  $\alpha$ . (b) same as (a) with the vertical scale enlarged. (c) The correlation of the best fit for  $\alpha$  and  $R_{non}$  and (d) The correlation of the best fit for  $\alpha$  and  $R_{res}$ .

### 1.3.4 Sensitivity to $B_s$ Mixing

BTeV can definitively reach  $x_s$  values of 75 in  $2 \times 10^7$  seconds of running. Put another way, it will take us only 10 days of steady running to reach  $x_s$  of 20. These estimates are based on the decay mode  $B_s \rightarrow D_s^+ \pi^-$ , with  $D_s^+ \rightarrow \phi \pi^+$  and  $K^{*0} K^+$ . “Definitively” is used here to express the ability to make a measurement where the best solution for a fit to the oscillation frequency is better by “5 standard deviations” than the next best fit. Thus BTeV can cover the entire range of  $x_s$  values allowed in the Standard Model.

### 1.3.5 Sensitivities in New Physics Modes

Precision studies of  $b$  decays can bring a wealth of information to bear on new physics, that probably will be crucial in sorting out anything seen at the LHC. While there are many tests for New Physics that we can make, we will concentrate on a few representative decay modes.

#### 1.3.5.1 Reach in Rare Decays

BTeV has excellent reach in rare decays. We have investigated the exclusive decays  $B^0 \rightarrow K^{*0} \mu^+ \mu^-$ ,  $B^+ \rightarrow K^+ \mu^+ \mu^-$  and the inclusive decay  $B \rightarrow X_s \mu^+ \mu^-$ .



Table 1.7: Results of Determining  $\alpha$  with 1000  $B^o \rightarrow \rho\pi$  Events.

$\alpha$ MC	Background, %		$\langle\alpha\rangle$	$\langle\sigma_\alpha\rangle$	$\langle\alpha\rangle$	$\langle\sigma_\alpha\rangle$
	Resonant.	Nonres.	1 parameter		3 parameters	
77.3	0	0	77.4	1.3	77.3	1.4
	10	10	77.4	1.4	77.3	1.5
	20	20	77.2	1.5	77.2	1.6
	40	0	77.4	1.6	77.2	1.8
	0	40	77.6	1.4	77.1	1.6
93.0	0	0	92.7	1.4	92.8	1.5
	10	10	93.3	1.6	93.4	1.8
	20	20	93.1	1.7	93.3	1.9
	40	0	92.7	1.8	93.2	2.1
	0	40	92.5	1.6	93.3	1.9
111.0	0	0	111.0	1.9	111.7	2.3
	10	10	110.7	2.3	110.6	3.6
	20	20	110.9	2.7	111.7	3.9
	40	0	111.2	2.8	110.4	4.3
	0	40	110.2	2.1	111.1	4.0

We acquire 2530  $K^{*o}\mu^+\mu^-$  decays in  $10^7$  seconds, with a signal/background of 11. This sample is enough to measure the lepton-forward-backward asymmetry and test the Standard Model. (We expect a similar number of  $K^{*o}e^+e^-$  events, but since we have not simulated these, we have not added them into our sample.) The Dalitz plot and forward-backward polarization are sensitive tests of New Physics. How sensitive they are depends on how much the New Physics differs from Standard Model expectations. In Fig. 1.18 we show the simulated data using the Standard Model expectation for the forward-backward asymmetry, assuming two years of dating taking using only  $K^{*o}\mu^+\mu^-$  or one year if  $K^{*o}e^+e^-$  are added in with the same acceptance. A fit to the data determines the location of the zero with a precision of 4%. This can be compared with the zero locations given in non-SM models as shown in Fig. 1.7 (unfortunately plotted here in terms of  $s$ , rather than  $\sqrt{s}$ ).

Although the asymmetry is expected to be small in  $K^+\mu^+\mu^-$ , we also test the Standard Model expectation, due to our large sample of  $\sim 1300$  events per year with a signal/background of 3.

We also expect to be able to measure the inclusive rate  $b \rightarrow s\mu^+\mu^-$  with  $20\sigma$  significance. This inclusive rate is very important. It could either show non-Standard Model physics or greatly constrain alternative models.

Other modes useful, for example, to test for Extra Dimensions are  $B_s \rightarrow \mu^+\mu^-$  and  $B_d \rightarrow \mu^+\mu^-$ , where we expect totals of six and one event, respectively in  $10^7$  seconds, with signal/background above 10.

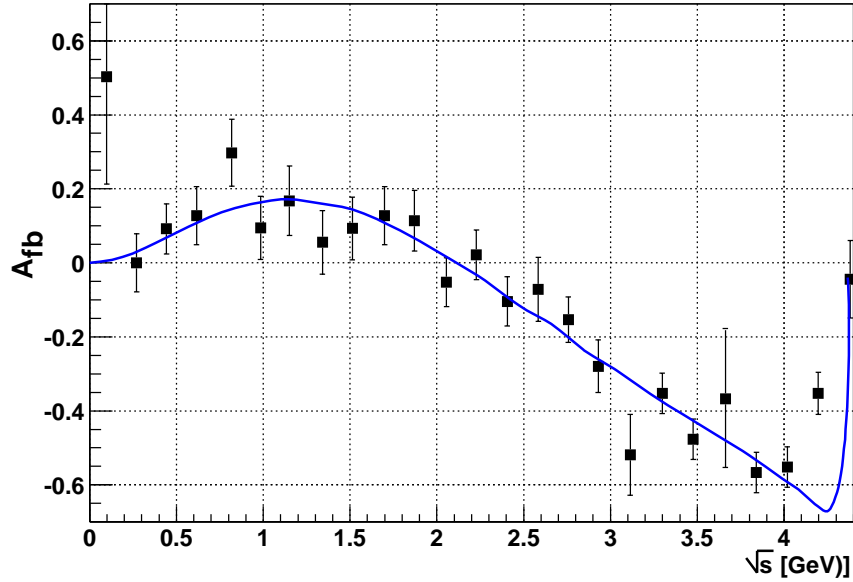


Figure 1.18: The normalized forward-backward asymmetry in  $B \rightarrow K^* \mu^+ \mu^-$  decay as a function of  $\sqrt{s}$ , the dilepton invariant mass. From ref. [56]

### 1.3.5.2 Reach in CP Violating Modes

The measurements described above of the CP violating angles and  $x_s$  already provide generic tests of New Physics. A large value of the angle  $\chi$ , above  $\sim 4^\circ$ , would already provide prima facie evidence of New Physics.

Many other CP violating decay modes are also useful in detecting New Physics. In Table 1.8 we present our yields and the sensitivity in a few of these modes.

Table 1.8: BTeV Sensitivities in CP Violating Modes Pointed Toward New Physics for  $10^7$  seconds

Mode	$\mathcal{B} \times 10^{-6}$	Yield	S/B	parameter	error
$B^- \rightarrow \phi K^-$	6.9	11000	>10	CP asymmetry	0.01
$B^0 \rightarrow \phi K_s$	3.45	2000	5.2	$\sin(2\beta)$	0.11
$D^{*+} \rightarrow \pi^+ D^0; D^0 \rightarrow K^- \pi^+$	$2.6 \times 10^4$	$\sim 10^8$	large	CP asymmetry	very small <sup>†</sup>

<sup>†</sup> Systematic error limited

The combination of measurements of all of these modes, the previous ones listed in Table 1.4 and many others than we can study with high statistics, will allow for a critical examination of any new physics found at the LHC.

## 1.4 Physics Reach of the Stage I Detector and Comparisons with LHCb

### 1.4.1 Introduction

The stage I detector has less physics reach than the full detector, yet there is plenty of physics it can do. In this section we will establish that it is fully competitive with LHCb, and that we will go well beyond LHCb when stage II is installed.

First of all let us take into account the reductions to our sensitivities due to the incomplete detector.

- Not having 50% of the  $\text{PbWO}_4$  crystals reduces our data rate for final states with  $\pi^0$ 's or  $\eta$ 's by about 50%.
- Not having 75% of the phototubes for the liquid radiator effectively renders this part of the RICH system inoperative causing a reduction of the flavor tagging efficiency by about 25%.
- Not having one muon tracking station and the dimuon trigger has almost no effect on our sensitivities because the dimuon trigger is used as a systematic check on the detached vertex trigger that is very important in the long run but not at the beginning of the experiment; muon identification is still excellent with just two stations as the third station is mainly for the trigger.
- Not having 50% of the trigger and DAQ capability mainly reduces our capacity to record direct charm events.
- Not having two of the seven tracking stations causes more ghost tracks and a slightly worsened momentum resolution.

Next, there is a further small reduction due to the change from the Tevatron staying at 396 ns bunch spacing rather than going to 132 ns, that increases the effective number of interactions per bunch by a factor of three. These effects are documented in the appendix to the TDR [75] and are taken here as an overall 10% reduction in effective rates.

The physics reach of the Stage I detector for an integrated luminosity of  $2 \text{ fb}^{-1}$  is shown in Table 1.9.

Table 1.9: Yearly sensitivities to CP violating angles and related quantities for the Stage I detector. ( $\mathcal{L} = 2 \times 10^{32} \text{cm}^{-2} \text{s}^{-1}$  for  $10^7$  s.) (Reactions between lines are used together.)

Reaction	$\mathcal{B} \times 10^{-6}$	# of Events	S/B	Parameter	Error (Value)
$B_s \rightarrow D_s^+ K^-$	300	6,750	7	$\gamma - 2\chi$	$9.4^\circ$
$B_s \rightarrow D_s^+ \pi^-$	3000	53,000	3	$x_s$	(72)
$B^0 \rightarrow J/\psi K_s$	445	151,000	10	$\sin(2\beta)$	0.02
$B^0 \rightarrow J/\psi K^0$					
$K^0 \rightarrow \pi^\pm \ell^\mp \nu$	7	225	2.3	$\cos(2\beta)$	$\sim 0.6$
$B^0 \rightarrow \pi^+ \pi^-$	4.5	13,100	3	Asymmetry	0.035
$B_s \rightarrow K^+ K^-$	17	17,000	6.6	Asymmetry <sup>†</sup>	0.024
$B^- \rightarrow \overline{D}^0 (K^+ \pi^-) K^-$	0.17	150	1		
$B^- \rightarrow \overline{D}^0 (K^+ K^-) K^-$	1.1	900	>10	$\gamma$	$13.6^\circ$
$B^- \rightarrow K_s \pi^-$	12.1	4,100	1		$< 5^\circ +$
$B^0 \rightarrow K^+ \pi^-$	18.8	55,900	20	$\gamma$	theory errors
$B^0 \rightarrow \rho^+ \pi^-$	28	2,430	4.1		
$B^0 \rightarrow \rho^0 \pi^0$	5	350	0.3	$\alpha$	$\sim 7^\circ$
$B_s \rightarrow J/\psi \eta$	330	1,260	15		
$B_s \rightarrow J/\psi \eta'$	670	4,400	30	$\sin(2\chi)$	0.040

<sup>†</sup> Can be used for a model dependent estimate of  $\gamma$ , see ref. [46].

# Bibliography

- [1] M. B. Gavela, P. Hernández, J. Orloff and O. Pène O, *Mod. Phys. Lett. A* **9**, 795 (1993) [hep-ph/9312215].
- [2] J. Ellis, Nucl. Phys. Proc. Suppl. **99A**, 331 (2000) [hep-ph/0011396].
- [3] M. Kobayashi and K. Maskawa *Prog. Theor. Phys.* 49, 652 (1973).
- [4] L. Wolfenstein *Phys. Rev. Lett.* 51, 1945 (1983).
- [5] J. P. Silva, L. Wolfenstein, *Phys. Rev. D* **55**, 5331 (1997) [hep-ph/9610208].
- [6] R. Aleksan, B. Kayser and D. London, *Phys. Rev. Lett.* **73**, 18 (1994) [hep-ph/9403341].
- [7] I. I. Bigi and A. I. Sanda, “On the Other Five KM Triangles,” [hep-ph/9909479].
- [8] Y. Nir, “CP Violation: The CKM Matrix and New Physics,” Plenary talk given at the 31st international conference on high energy physics (ICHEP 2002), Amsterdam, 24-31 July 2002, [hep-ph/0208080].
- [9] S. Stone, “Experimental Results in Heavy Flavor Physics,” Plenary talk at International Europhysics Conference on High Energy Physics EPS (July 17th-23rd 2003) in Aachen, Germany, to appear in the Proceedings [hep-ph/0310153].
- [10] A. Hocker *et al.*, *Eur. Phys. J. B* **435**, 427 (1998).
- [11] M. E. Peskin, “Theoretical Summary Lecture for EPS HEP99,” to appear in proceedings [hep-ph/0002041].
- [12] F. J. Greub, A. Ioannissian and D. Wyler, *Phys. Lett. B* **346**, 149 (1995) [hep-ph/9408382].
- [13] A. Masiero and O. Vives, “New Physics Behind the Standard Model’s Door?,” Int. School on Subnuclear Physics, Erice, Italy, 1999 [hep-ph/0003133].
- [14] Y. Nir, “CP Violation In and Beyond the Standard Model,” IASSNS-HEP-99-96 [hep-ph/9911321] (1999).

- [15] I. Hinchliff and N. Kersting, “Constraining CP Violating Phases of the MSSM,” *Phys. Rev. D* **63**, 015003 (2001) [hep-ph/0003090].
- [16] R. A. Briere *et al.*, *Phys. Rev. Lett.*, **86**, 3718 (2001) [hep-ex/0101032].
- [17] B. Aubert *et al.*, *Phys. Rev. Lett.*, **87**, 151801 (2001) [hep-ex/0105001].
- [18] A. Ali *et al.*, *Phys. Rev. D* **61**, 074024 (2000) [hep-ph/9910221].
- [19] A. Ali *et al.*, *Phys. Rev. D* **66**, 034002 (2002) [hep-ph/0112300].
- [20] D. Chakraverty, K. Huitu and A. Kundu, “Effects of Universal Extra Dimensions on  $B^0$  Mixing,” [hep-ph/0212047]; J. Kubo and H. Terao, Suppressing FCNC and CP-Violating Phases with Extra Dimensions [hep-ph/0211180]; S. J. Huber, “Flavor Physics and Warped Extra Dimensions,” [hep-ph/0211056]; K. Agashe, N. G. Deshpande and G. H. Wu, “Universal Extra Dimensions and  $b \rightarrow s\gamma$ ,” *Phys. Lett. B* **514**, 309 (2001) [hep-ph/0105084]; G. Barenboim, F. J. Botella and O. Vives, “Constraining Models With Vector-Like Fermions from FCNC in K and B Physics,” *Nucl. Phys. B* **613**, 285 (2001) [hep-ph/01050306]; G. C. Branco, A. de Gouvea and M. N. Rebelo, “Split Fermions in Extra Dimensions and CP Violation,” *Phys. Lett. B* **506**, 115 (2001) [hep-ph/0012289]; D. Chang, W. Y. Keung and R. N. Mohapatra, “Models for Geometric CP Violation With Extra Dimensions,” *Phys. Lett. B* **515**, 431 (2001) [hep-ph/0105177]; J. Papavassiliou and A. Santamaria, “Extra Dimensions at the One Loop Level:  $Z \rightarrow b\bar{b}$  and  $B - \bar{B}$  Mixing,” *Phys. Rev. D* **63**, 016002 (2001) [hep-ph/016002].
- [21] A. Aranda and J. Lorenzo Diaz-Cruz, “Flavor Symmetries in Extra Dimensions,” [hep-ph/0207059].
- [22] A. J. Buras, M. Spranger and A. Weiler, “The Impact of Universal Extra Dimensions on the Unitarity Triangle and Rare  $K$  and  $B$  Decays,” [hep-ph/0212143].
- [23] T. Appellequist, H.C. Cheng and B. A. Dobrescu, *Phys. Rev. D* **64**, 035002 (2001) [hep-ph/0012100].
- [24] D. Chang, A. Masiero and H. Murayama, “Neutrino mixing and large CP violation in  $B$  physics,” [hep-ph/0205111].
- [25] L. Wolfenstein and Y.L. Wu, *Phys. Rev. Lett.* **74**, 2809 (1994) [hep-ph/9410253].
- [26] G. Buchalla, G. Hiller, and G. Isidori, *Phys. Rev. D* **63**, 014015 (2000) [hep-ph/0006136].
- [27] I. Hinchliff and N. Kersting, “CP Violation from Noncommutative Geometry,” LBNL-47750 [hep-ph/0104137].
- [28] A. Bartl, *et al.*, *Phys. Rev. D* **64**, 076009 (2001) [hep-ph/0103324].

- [29] A. Ali, G. Kramer and C. D. Lu, *Phys. Rev.* **D 59**, 014005 (1999) [hep-ph/9805403].
- [30] B. Kayser, “Cascade Mixing and the CP-Violating Angle Beta,” [hep-ph/9709382]. Previous work in this area was done by Y. Azimov, *Phys. Rev.* **D 42** (1990) 3705.
- [31] A. Dighe, I. Dunietz and R. Fleischer, *Phys. Lett.* **B 433**, 1998 (147) [hep-ph/9804254].
- [32] A. E. Snyder and H. R. Quinn, *Phys. Rev.* **D 48** (1993) 2139.
- [33] C. P. Jessop *et al.* (CLEO), *Phys. Rev. Lett.*, **85**, 2881 (2000) [hep-ex/0006008].
- [34] M. Bona, BABAR preprint BABAR-CONF-01/71, SLAC-PUB-9045 [hep-ex/0107058].
- [35] B. Aubert *et al.* (Babar), [hep-ex/0311049].
- [36] A. Gordon *et al.* (Belle), *Phys. Lett. B*, **542**, 183 (2002) [hep-ex/0207007].
- [37] A. Ali, G. Kramer, and C.D. Lu, *Phys. Rev.* **D 59**, 014005 (1999) [hep-ph/9805403].
- [38] Y. Grossman and H. R. Quinn, *Phys. Rev.* **D 56**, 7259 (1997) [hep-ph/9705356].
- [39] D. Du, I. Dunietz and Dan-di Wu, *Phys. Rev.* **D 34**, 3414 (1986); R. Aleksan, I Dunietz, and B. Kayser, *Z. Phys.* **C 54**, 653 (1992); R. Aleksan *et al.*, *Z. Phys.* **C 67**, 251 (1995) [hep-ph/9407406].
- [40] D. Atwood, I. Dunietz and A. Soni, *Phys. Rev. Lett.* **78**, 3257 (1997).
- [41] M. Gronau and D. Wyler, *Phys. Lett.* **B 265**, 172 (1991).
- [42] R. Fleischer and T. Mannel, *Phys. Rev.* **D 57**, 2752 (1998) [hep-ph/9704423].
- [43] M. Neubert and J. L. Rosner, *Phys. Rev. Lett.* **81**, 5076 (1998) [hep-ph/9809311].
- [44] A. J. Buras and R. Fleischer, “Constraints on  $\gamma$  and Strong Phases from  $B \rightarrow \pi K$  Decays,” presented at ICHEP 2000, Osaka, Japan, July 2000. To appear in the Proceedings [hep-ph/0008298].
- [45] M. Beneke, G. Buchalla, M. Neubert and C. T. Sachrajda, “QCD factorization for  $B \rightarrow \pi K$  decays,” Contribution to ICHEP 2000, July 2000, Osaka, Japan, to appear in the Proceedings [hep-ph/0007256].
- [46] R. Fleischer, *Eur. Phys. J.* **C10** 299, 1999.
- [47] G. Hiller, “Physics Reach of Rare  $B$  Decays,” [hep-ph/0207121].
- [48] A. Masiero and O. Vives, New Physics in CP Violation Experiments, *Ann. Rev. of Nucl. & Part. Science* **51**, (2001) [hep-ph/0104027].

- [49] V. Kostelecky and R. Van Kooten, *Phys. Rev. D*, **54**, 5585 (1996) [hep-ph/9607449]; Dong-Sheng Du and Zheng-Tao Wei, *Eur. Phys. J.*, **C14**, 479 (2000) [hep-ph/9904403]; L. Lavoura, *Phys. Rev. D*, **62**, 056002 (2000) [hep-ph/9911209], and references cited therein.
- [50] <http://www-btev.fnal.gov/DocDB/0000/000066/002/index.html>
- [51] I. Dunietz, *Phys. Lett. B* **427**, 179 (1998) (hep-ph/9712401).
- [52] A. E. Snyder and H. R. Quinn, *Phys. Rev. D* **48** (1993) 2139.
- [53] H. R. Quinn and J. P. Silva, “The Use of Early Data on  $B \rightarrow \rho\pi$  Decays,” hep-ph/0001290 (2000).
- [54] K. Abe *et al.*, *Phys. Rev. Lett.* **88**, 021801 (2002) (hep-ex/0109026).
- [55] <http://www-btev.fnal.gov/public/hep/general/proposal/index.shtml>
- [56] G. Burdman, *Phys. Rev. D.*, **57**, (1998) (hep-ph/9710550).
- [57] See *B Decays, revised 2nd Edition* ed. S. Stone, World Scientific, Singapore, (1994).
- [58] B. Aubert *et al.*, *Phys. Rev. Lett.* **87**, 091801 (2001), *ibid.* **86**, 2525 (2001), and B. Aubert *et al.*, “A Study of Time-Dependent CP-Violating Asymmetries and Flavor Oscillations in Neutral B Decays at the Upsilon(4S),” (hep-ex/0201020) (2002); K. Abe *et al.*, *Phys. Rev. Lett.* **87**, 091802 (2001).
- [59] B. Aubert *et al.* (BABAR), “Study of CP-violating asymmetries in  $B^0 \rightarrow \pi^+\pi^-$ ,  $K^+\pi^-$  decays,” (hep-ex/0110062) (2001).
- [60] Z. Zhao *et al.*, “Report of Snowmass 2001 Working Group E2: Electron-positron Colliders from the  $\phi$  to the Z,” to appear in the proceedings (hep-ex/0201047).
- [61] S. Henderson, “M2: Summary -Electron-Positron Circular Colliders,” presented at Snowmass 2001, to appear in the proceedings, [http://vmsstreamer1.fnal.gov/VMS\\_Site\\_02/Lectures/Snowmass2001/720M2Henderson/sld016.htm](http://vmsstreamer1.fnal.gov/VMS_Site_02/Lectures/Snowmass2001/720M2Henderson/sld016.htm)
- [62] DOE/NSF HIGH-ENERGY PHYSICS ADVISORY PANEL SUBPANEL ON LONG RANGE PLANNING FOR U.S. HIGH-ENERGY PHYSICS, available at <http://doe-hep.net/>.
- [63] P. Ball *et al.*, “B decays at the LHC,” CERN-TH/2000-101 (hep-ph-0003238).
- [64] K. Abe *et al.*, (CDF), *Phys. Rev. Lett.* **75**, 1451 (1995); S. Abachi *et al.*, (D0), *Phys. Rev. Lett.* **74**, 3548 (1995). See also the UA1 measurement C. Albajar *et al.*, *Phys. Lett. B* **186**, 237 (1987); **B213**, 405 (1988); **B256**, 121 (1991).



- [65] K. Abe *et al.*, (CDF), *Phys. Rev. Lett.* **76**, 4462 (1996); *ibid* **77**, 1945 (1996); K. Abe *et al.*, (CDF), *Phys. Rev. D* **57**, 5382 (1998).
- [66] T. Junk, “A Review of  $B$  Hadron Lifetime Measurements from LEP, the Tevatron and SLC,” in Proceedings of the 2nd Int. Conf. on *B Physics and CP Violation*, Univ. of Hawaii, (1997), ed. T. E. Browder *et al.*, World Scientific, Singapore (1998).
- [67] K. Abe *et al.*, (CDF), “Observation of  $B_c$  Mesons in  $p - \bar{p}$  Collisions at  $\sqrt{s} = 1.8$  TeV,” hep-ex/9804014 (1998).
- [68] M. Paulini, “B Lifetimes, Mixing and CP Violation at CDF,” Review article to appear in the Int. Journal of Modern Physics A, hep-ex/9903002 (1999).
- [69] K. Anikeev *et al.*, “ $B$  Physis at the Tevatron: Run II and Beyond,” FERMILAB-PUB-01/197 (hep-ph/0201071) (2001).
- [70] “LHCb Technical Proposal,” CERN/LHCC 98-4, LHCC/P4 (1998), available at <http://lhcb.cern.ch> .
- [71] See T. Nakada, “LHCb Light status and related issue,” at <http://lhcb-doc.web.cern.ch/lhcb-doc/progress/progress.htm>
- [72] We have confirmed with T. Nakada, the LHCb spokesperson, that the yields for this mode as quoted in their Technical Proposal are their current values that we should use in our comparisons. The branching ratio numbers used by LHCb were taken from Table 15.11 on page 157. The number of events were taken from Table 15.12. Since these numbers are quoted as being “tagged,” we divided by the 0.40 tagging efficiency given on page 145. The two final states  $\rho^+\pi^-$  and  $\rho^-\pi^+$  are given separately by LHCb; we added them together. The same procedure was followed for  $B_s \rightarrow D_s K$ .
- [73] P. Ball *et al.*, “ $B$  Decays at the LHC,” CERN-TH/2000-101, hep-ph/0003238.
- [74] Although they state a 1% efficiency here, this is only a partial efficiency according to T. Nakada.
- [75] <http://www-btev.fnal.gov/DocDB/0021/002115/011/index.shtml>